ARTICLE IN PRESS

Available online at www.sciencedirect.com

ScienceDirect

Quaternary International ▮ (▮▮▮▮) ▮▮▮–▮▮▮

Spatial and temporal variation of runoff in the Yangtze River basin during the past 40 years

Jijun Xu[a,b], Dawen Yang[a,*], Yonghong Yi[a], Zhidong Lei[a], Jin Chen[b], Wenjun Yang[b]

[a]*State Key Laboratory of Hydro-science and Engineering, Tsinghua University, Beijing 100084, China*
[b]*Changejiang Scientific Research Institute, Wuhan 430010, China*

Abstract

Frequent floods occur in the Yangtze River basin, where the Three Gorges reservoir has been constructed. However, in recent years, it has been found that droughts have also occurred frequently. For a better understanding of the spatial and temporal variations in runoff in the Yangtze River basin, especially in the upper Three Gorges reservoir area during the past 40 years, a hydro-climate data analysis was carried out together with rainfall-runoff modeling. The trends in precipitation and river discharge were analyzed for the whole Yangtze River basin, offering a comparison upstream and downstream of the Three Gorges Dam. The results showed that both precipitation and discharge along the downstream of the dam had statistically significant increasing trends in summer. However, the upstream area had significant decreasing trends for both precipitation and discharge in autumn. To analyze the spatial-temporal variation of runoff in the upper Yangtze River, a geomorphology-based distributed hydrological model (GBHM) was used for simulating the natural runoff during 1961–2000. It was confirmed that the natural runoff increased in summer and decreased greatly in autumn. This natural change in runoff in the upper Yangtze River basin implies an increasing flood risk in summer and water shortage in autumn.

1. Introduction

An important factor that should be taken into account for river basin management is the spatial and temporal variability in runoff under global climate change. Climate change will accelerate the water cycle and bring more precipitation as well as runoff on a global scale (Houghton et al., 2001). However, shifts of precipitation in space and time have brought about more frequent floods and droughts throughout the world (Trenberth et al., 2003; Milly et al., 2005), and will continue in the 21st century. Especially, the seasonal and regional changes in runoff might upset the vulnerable balances not only between natural disasters and the existing engineering counter-measures but also between the human water demand and water resource availability.

There has been considerable research addressing the influences of the climate change on the precipitation and streamflow in the Yangtze River. The change trends of temperature, precipitation and streamflow and their extremes have been examined based on observed data at meteorological and hydrological gauges (Gemmer et al., 2004; Zhang et al., 2005; Becker et al., 2006; Su and Jiang, 2006; Jiang et al., 2007). Previous studies concluded that extreme precipitation events have increased, and this has intensified the flood hazards as well as droughts. Particularly in the middle and lower reaches of the Yangtze River, the observed annual maximum streamflow has a significant upward trend (Zhang et al., 2006b).

There have also been many papers emphasizing the impacts of human activities on the streamflow. Chen et al. (2001) examined the human impacts on the major hydrological processes in the Yangtze River basin, with a special focus on the influence on the discharge from the drainage basin to the sea during the dry season according to observed data and related statistical information. The results indicated that the decrease in vegetation cover and the increase in reservoir capacity have also impacted water discharge over the past decades. For detecting changes in

*Corresponding author.
E-mail address: yangdw@tsinghua.edu.cn (D. Yang).

1040-6182/$ - see front matter © 2007 Elsevier Ltd and INQUA. All rights reserved.
doi:10.1016/j.quaint.2007.10.014

the seasonal water discharge and sediment load in the upper Yangtze, Lu et al. (2003) demonstrated that seasonal data were more useful than aggregated annual values in a monsoon climate, and suggested that the significant increases in sediment load in wet seasons and decreases in water flow in dry seasons (e.g. in the Dadu tributary) were due to deforestation. They found that the inconsistency between changes in water flow and sediment load (e.g. in the Min tributary) was predominantly due to water consumption. Zhang et al. (2006a) stated that human activities (deforestation, dam construction and operation, etc.) exert more influences on sediment loads than on annual runoff, and indicated that the variation in the annual runoff was mainly controlled by climate fluctuation (i.e. precipitation variation).

However, by only analyzing the changes in observed precipitation and streamflow, it is difficult to sufficiently relate hydrological changes to a climatic signal and segregate the possible direct human impact, because of the nonlinear behavior of hydrological processes as well as the impact of dam construction, land-use changes and irrigation. Changes in precipitation cannot easily be converted into amounts of streamflow change. Generally, the observed discharge is an integrated indicator of the hydrological response of the drainage area above the gauge, which is not only closely connected to the climate but also to the topography, river, soil, geology and vegetation. Changes in climate and vegetation induce changes in a hydrological cycle and the change in river discharge as a result. In addition, hydraulic structures on the rivers, such as high dams and large reservoirs, can change the river flow to a large extent.

Therefore, for a better understanding of the change in a watershed hydrological cycle, not only is it necessary to know the natural response of the streamflow to climatic change but also to quantify the impacts of human activities on river runoff. Obviously, trend analysis based on the observed data is inadequate, and a new approach or tool is required. Hydrological models have been used widely for water resource assessment, especially for studying the impact of climate change (Oki et al., 2001; Doll et al., 2003). The distributed, physically based hydrological models have potentially more correct descriptions of the hydrological processes than do the other model types. Furthermore, they have the advantage of using spatial information supported by GIS and remote-sensing techniques (Refsgaard, 1996).

Based on the previous studies, this study assesses the trends in precipitation and river discharge using the available gauge records. A distributed physically based hydrological model is employed for simulating the ‘‘natural river discharge’’ together with the available geographic information of topography, land cover and vegetation in the upper Yangtze River basin. Incorporating the simulated results into the observed river discharge data, the present paper aims to provide a quantitative analysis of the spatial and temporal variations in runoff and a better understanding of the relationship between the change trends in the precipitation and river discharge.

2. Study area and data description

2.1. Study area

The Yangtze River, also called Changjiang in Chinese, is the longest (also the largest) river basin in China, and the third longest river in the world. It originates from the Tibetan Plateau, crosses the country from the west to the east and finally flows into the East China Sea. The Yangtze River flows about 6300 km in distance and has 1.8 million km^2 of drainage area. Nearly 440 million people live in this river basin. The upstream of the Yichang gauge (see Fig. 1, near the Three Gorges Dam site) is called the upper Yangtze River and has a drainage area of about 1.0 million km^2, and contains four major tributaries, named Yalongjiang, Minjiang, Jialingjiang and Wujiang. The middle part of the upstream is the Sichuan basin where the elevation is lower than 1000 m (see Fig. 1b). The region between the Yichang gauge and Jiujiang gauge is called the middlestream, which includes the Hanjiang tributary and two large lakes, named Dongting Lake and Poyang Lake. Below the Jiujiang gauge is the lower Yangtze River. The long-term mean of the annual precipitation in the Yangtze River basin is about 1070 mm, but the spatial and temporal distributions are highly uneven. The annual spatial precipitation ranges from 500 mm in the west to 2500 mm in the east, and more than 60% of annual precipitation is concentrated in summer (June, July and August). This climate causes floods frequently as well as droughts sometimes in the river basin.

The upper Yangtze River is abundant in hydropower potential, and intensive development of hydropower is now ongoing. Moreover, the tributaries of Yalongjiang and Minjiang have also been proposed as source areas for the west route of the south–north water transfer project. After the construction of the Three Gorges Dam and other large-scale hydraulic structures on the mainstream and tributaries, the river flow will be disturbed greatly in the near future. Therefore, an accurate water resource assessment and flood forecast will become more and more important for the operation of reservoirs as well as for water resource allocation.

2.2. Data description

The daily climatic dataset from the China Meteorological Administration (CMA) was used. The daily meteorological data are available at 154 stations inside the Yangtze River basin. The weather parameters include precipitation, mean air temperature, minimum and maximum air temperature, wind speed, relative humidity and sunshine time. The daily discharge data are collected from the ‘‘Hydrological Year Book’’ published by the Hydrological Bureau of the Ministry of Water Resources of

Please cite this article as: Xu, J., et al., Spatial and temporal variation of runoff in the Yangtze River basin during the past 40 years. Quaternary International (2007), doi:10.1016/j.quaint.2007.10.014

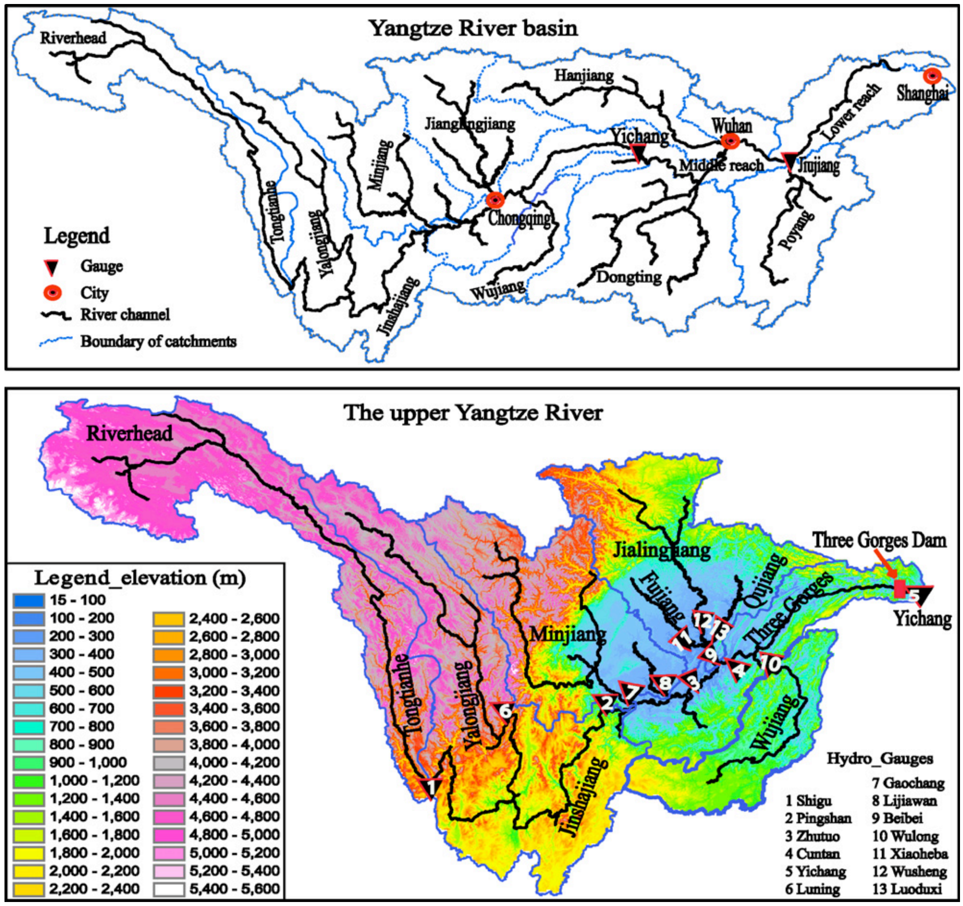

Fig. 1. Study area: (a) whole Yangtze River basin and (b) upper Yangtze River.

China. In this study, 26 hydrological gauges located on the mainstream and the major tributaries are selected. Because most meteorological stations and hydrological gauges were built in the 1950s, the available time series of these data are from 1961 to 2000.

For building the distributed hydrological model, the digital elevation data and relevant geographical information data have been used. The DEM is obtained from the global topography database (http://telascience.sdsc.edu/tela_data/SRTM/version2/SRTM3/), which has a 3 arc-second spatial resolution. In this study, the digital elevation model (DEM) is re-sampled to a 100 m resolution using the Lambert projection coordinate system. A land use map is obtained from the USGS Global Land Cover Characteristics Database (Version 2.0) with a 1 km spatial resolution (http://edc.usgs.gov/glcc/globe_int.html), and is reclassified into 10 types, including water body, urban area, bare soil, grassland, forest, paddy filed, upland, shrub, wetland and snow. For each vegetation type, a monthly leaf-area-index (LAI) is calculated from the monthly Normalized Difference Vegetation Index (NDVI). A global dataset of monthly NDVI with an 8 km resolution is obtained from the DAAC of GSFC/NASA (http://daac.gsfc.nasa.gov). This dataset has been available since 1981. A soil map is obtained from FAO/UNESCO with a 10-km resolution, and the soil–water parameters are obtained from the global soil data products of IGBP-DIS (http://www.daac.ornl.gov), in which the same soil classification as for the FAO/UNESCO data has been used.

3. Precipitation and river discharge trend detection

3.1. Method of trend significance test

The Mann–Kendall non-parametric test has been recommended as an excellent tool for trend detection. The present study applies this test for detecting the significance of the trends in annual, seasonal and monthly meteorological and hydrological time series. To eliminate the influence of a serial correlation on the Mann–Kendall (MK) test, Kulkarni and von Storch (1995) proposed to pre-whiten a series prior to applying the MK test. For a more effective reduction of the effect of serial correlation on the MK test, a modified pre-whitening procedure, termed trend-free pre-whitening (TFPW), was proposed by Yue et al. (2002), Yue and Wang (2002).

In this study, the approach of TFPW has been adopted to eliminate the influence of serial correlation of hydrological and meteorological data series before applying the MK test, and the significance level of the trend test a is set as 0.05.

3.2. Trends in precipitation and river discharge during 1961–2000

The trends of annual precipitation at 33 weather stations have passed the test at an $a = 0.05$ significance level. Among them, 26 weather stations have a statistically significant increasing trend, and are distributed mainly in the upstreams of the Poyang Lake and Dongting Lake, and in the Yalongjiang sub-basin (see Fig. 2a). However, 7 stations in the Sichuan Basin have a significant decreasing trend. The seasonal and monthly precipitations of the stations in the upstream of the Three Gorges Dam site showed different trends from the middle and lower reaches of the dam site. The precipitations at some stations located in the middle and lower reaches have a significant increasing trend in summer (namely June, July and August) (see Fig. 2b). This increasing trend in these areas was more significant in July (see Fig. 2d). However, the precipitation at many stations upstream of the dam site showed a significant decreasing trend in spring (namely March, April and May) and autumn (namely September, October and November), especially in the Sichuan Basin (see Figs. 2c and e).

The annual river discharges at hydrological gauges on the mainstream show no significant trend (see Fig. 2a). Chen et al. (2001) and Lu (2005) also presented similar results on the annual discharges. However, the seasonal and monthly changes in river discharge are more marked. The monthly river discharge observed at the Datong gauge on the mainstream of the lower reach in July increased greatly during 1961–2000 (see Fig. 3a), which may be due to the significant increase in rainfall in the middle and lower reaches at the same period. Zhang et al. (2006a) also found that the observed maximum discharge at the Datong gauge had a significant increasing trend during 1951–2000. This may imply an increase in the flood risk that exists in the middle and lower reaches.

The trends of observed river discharges are found to be more statistically significant on the tributaries than on the mainstream. Along the upper Yangtze River, the river discharges in autumn show a more significant decreasing trend, especially on the Minjiang and Jialingjiang tributaries (see Figs. 2c and e). For some relatively smaller branches, the decrease in river discharge in autumn is more marked. For example, the monthly mean discharge in September at the Luoduxi gauge in the Qujiang river, one branch of the Jialingjiang tributary, declined greatly since the 1990s (see Fig. 3b). The water consumption and reservoir regulation may be the predominante factors (Lu et al., 2003).

Table 1 gives a description of the detected gauges and their located drainage areas. Table 2 lists the area-averaged precipitation and the change trend in the upper Yangtze River and main tributaries. For the whole upper Yangtze River basin (above the Yichang gauge), the area-averaged annual precipitation is 840 mm. The annual precipitation in the riverhead area (above the Shigu gauge) is less than 504 mm. In the Minjiang sub-basin (above the Gaochang gauge), the Wujiang sub-basin (above the Wulong gauge) and the Qujiang sub-basin (above the Luoduxi gauge), the area-averaged annual precipitations are larger than 1000 mm. Table 3 lists the annual river discharge in water depth averaged over the drainage area and its change trend in the mainstream and major tributaries. It can be observed that the annual river discharge is largely determined by the amount of precipitation. The annual river discharge in the upper Yangtze River basin is about 435 mm. There is only 182 mm in the river discharge in the Tongtianhe tributary and the riverhead area. In both the Minjiang and the Wujiang tributaries, the area-averaged annual river discharges are more than 600 mm.

From Tables 2 and 3, it can be found that most of the change trends in the discharge are assorted with trends in the precipitation especially in autumn. In autumn, both the precipitation and the discharge show a significant decreasing trend, particularly the Minjiang and the Jialingjiang. In September, the precipitation and discharge in Tuojiang (noted as the Lijiawan guage), the Jialingjiang (noted as the Xiaoheba and Beibei gauges), the Qujiang (noted as the Luoduxi guage) and the Fujiang (noted as the Wusheng gauge) also had significant decreasing trends. The similar trend in the precipitation and the river discharge on these tributaries demonstrates that the dominant factor for the discharge decrease in September is the reduction of precipitation instead of human activity.

However, there are also some stations with different trends in the precipitation and discharge. For example, at the Luoduxi station, the annual discharge is significantly decreasing, but its precipitation shows a slightly increasing trend. At Wulong station, the annual river discharge increases while the precipitation is slightly decreasing. This inconsistency between the trends of the precipitation and river discharge also exists in the seasonal and monthly observations. The reason behind this phenomenon is not yet clear, and may be caused by the artificial regulation (e.g. reservoir operation) and/or changes in land use and cover.

4. Hydrological modeling in the upper Yangtze River Basin

4.1. Brief introduction of the GBHM model

The present study employs a distributed hydrological model (GBHM, geomorphology-based hydrological model) developed by Yang et al. (1998, 2002) for simulating the "natural runoff", in which only natural hydrological processes are included (there is no consideration of irrigation and reservoir control). The model uses a grid system with a 10-km spatial resolution, and runs in hourly time steps. The methodology used for constructing this model includes a sub-grid parameterization scheme, a basin sub-division scheme, a physically based hillslope hydrological simulation and a kinematic wave flow-routing method. The land surface conditions considered in the

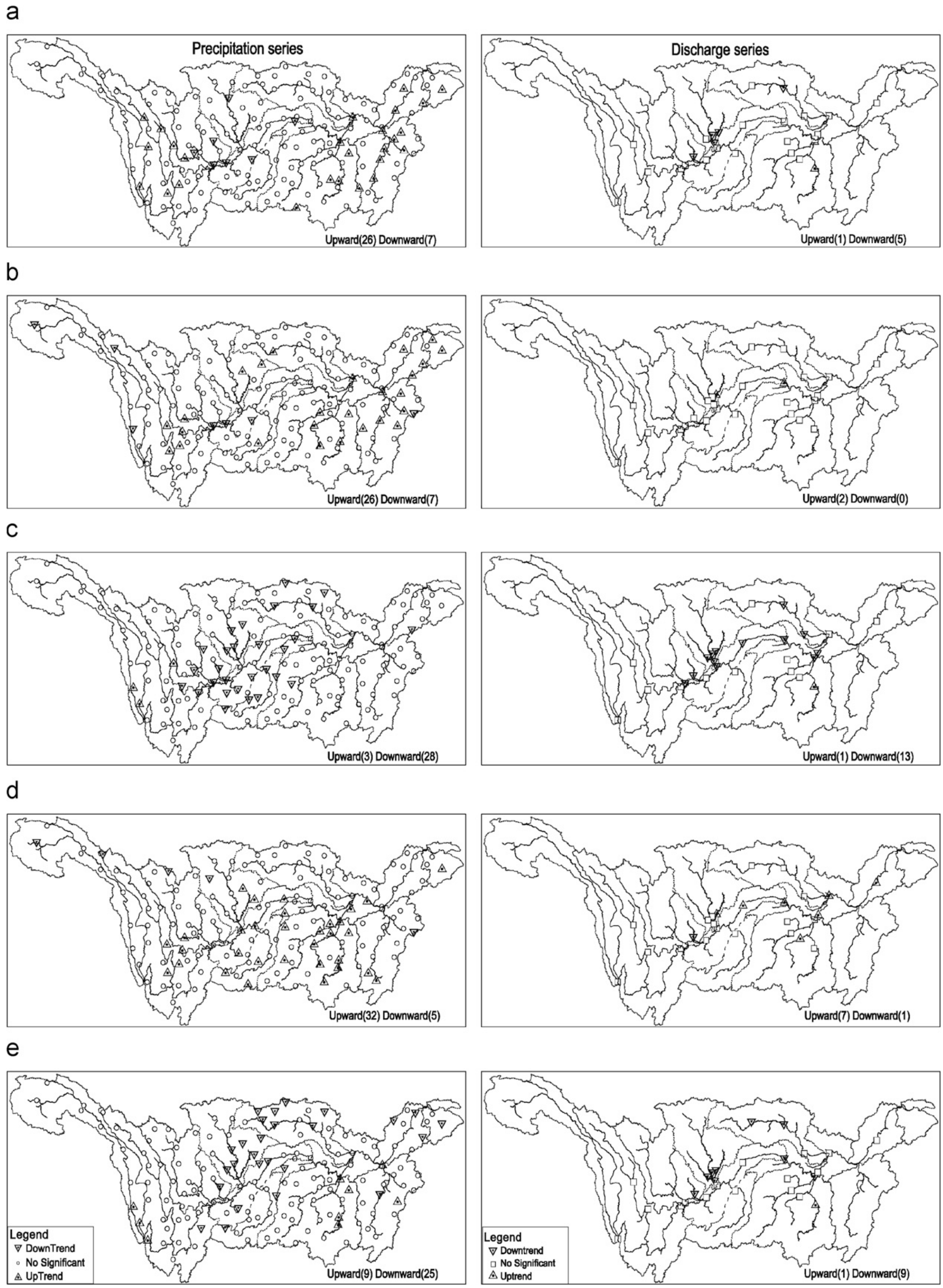

Fig. 2. Trends in precipitation and river discharge during 1961–2000: (a) annual, (b) in summer, (c) in autumn, (d) in July and (e) in September.

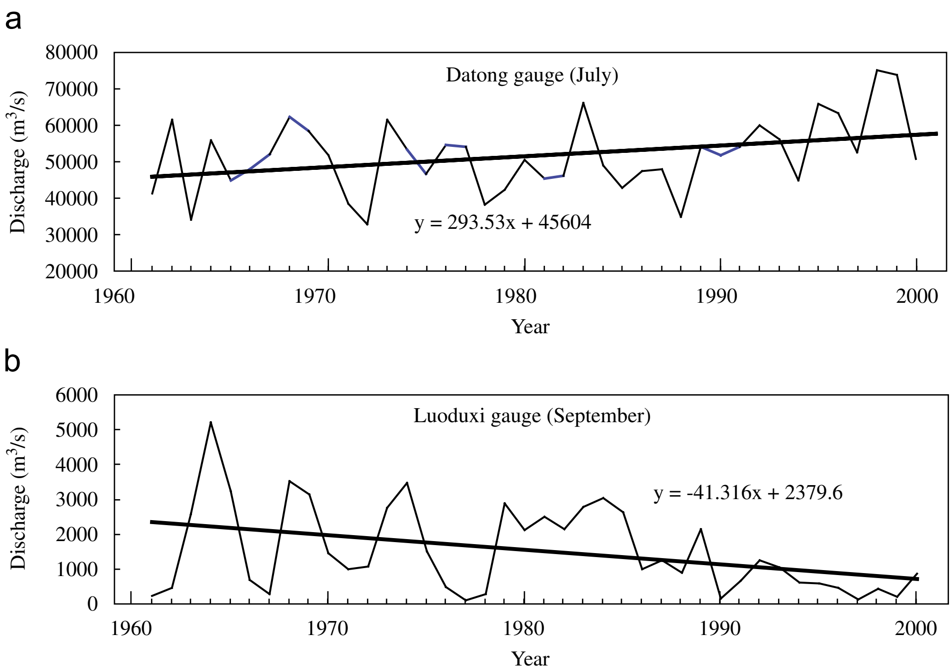

Fig. 3. Observed monthly river discharge: (a) at the Datong gauge on the mainstream of the lower reach and (b) at the Luoduxi gauge on the Qujiang tributary of the upper reach.

Table 1
Description of the gauges and their located drainage areas

Gauges	Location	Drainage area (km^2)
Shigu	Mainstream	232,600
Pingshan	Mainstream	458,800
Zhutuo	Mainstream	694,700
Cuntan	Mainstream	866,600
Yichang	Exit of the upper YR	1,005,500
Huning	On the Yalongjiang	108,000
Gaochang	Outlet of the Minjiang	132,600
Lijiawan	Outlet of the Tuojiang	23,200
Beibei	Outlet of the Jialingjiang	157,900
Wulong	Outlet of the Wujiang	83,000
Xiaoheba	Outlet of the Fujiang	29,400
Wusheng	Outlet of the Jialing	79,700
Luoduxi	Outlet of the Qujiang	38,100

hydrological simulation include the topography, land use, vegetation and soil. The atmospheric forcing used in the hydrological simulation is taken from a daily historical climate dataset.

The catchment is the minimum unit for implementing water resource management. For a large river basin, it needs to be sub-divided into sub-basins and to simulate the variability of water resources in each sub-basin. For sub-dividing the upper Yangtze River basin, the Pfafstetter scheme (Yang et al., 2000) is applied in the present study. In the present application, a total of 177 sub-basins have been identified upstream of the Yichang gauge. Since the model uses a 10-km grid, the heterogeneity inside a grid affects the hydrological processes, and therefore, a sub-grid parameterization is necessary. The sub-grid parameterization used in this research includes representations of the sub-grid variabilities in topography and land cover. The topographical parameterization uses the catchment geomorphologic properties, and represents a grid by a number of hillslopes. The hillslopes located in a 10-km grid are grouped according to the land cover types. The hydrological simulation is carried out for each land cover group. The hillslope is a fundamental computational unit for hydrological simulation. A physically based model is used for simulating the hillslope hydrology. The hydrological processes included in this model are snowmelt, canopy interception, evapotranspiration, infiltration, surface flow, sub-surface flow and the exchange between the groundwater and the river (Yang et al., 2002). The actual evapotranspiration is calculated from the potential evaporation by considering the seasonal variation of the LAI, root distribution and soil moisture availability. It is computed individually from the canopy water storage, root zone and soil surface. Infiltration and water flow in the sub-surface in the vertical direction and along the hillslope are described in a quasi-two-dimensional sub-surface model. The vertical water flow in the topsoil is represented by Richards' equation and solved by an implicit numerical solution scheme. In this scheme, the topsoil is sub-divided into a number of layers. Similar to the common sub-division used in many land surface schemes, the topsoil is divided into a near-surface layer of 5 cm, a root zone and a deep zone. The root zone and deep zone are again divided into sub-layers in the present model. The first layer is expected to be saturated during the rainfall period. Therefore, the upper boundary condition is

Table 2
The observed area-averaged precipitation and its trends in the upper Yangtze River

Gauges	Annual		Summer		Autumn		Jul		Sep	
	Mean (mm)	β (mm/a)	Mean (mm)	β (mm/a)	Mean (mm)	β (mm/a)	Mean (mm)	β (mm/a)	Mean (mm)	β (mm/a)
Shigu	503.73	0.49	310.28	−0.54	99.25	**0.64**	107.77	−0.04	70.71	**0.37**
Pingshan	671.11	**0.83**	403.82	0.08	149.53	0.37	142.97	**0.36**	97.76	0.28
Zhutuo	768.42	−0.01	442.78	−0.31	166.57	0.09	155.11	**0.17**	105.76	0.14
Cuntan	799.77	−0.46	444.04	−0.08	180.86	**−0.38**	160.60	0.20	111.92	**−0.18**
Yichang	839.55	−0.49	450.16	0.31	191.03	**−0.52**	162.10	0.37	112.42	**−0.26**
Huning	763.18	1.15	454.59	0.62	173.98	0.29	160.22	**0.47**	118.10	0.17
Gaochang	1019.5	−1.64	538.20	−1.23	204.08	−0.13	179.06	−0.33	126.46	0.01
Lijiawan	974.53	**−3.47**	552.53	−2.19	213.60	**−1.65**	212.04	−0.93	131.94	**−0.87**
Beibei	887.97	−1.96	443.11	0.65	226.56	**−2.03**	182.09	0.19	136.72	**−1.41**
Wulong	1128.64	−0.65	515.75	2.82	250.68	**−1.49**	174.58	1.42	107.96	−0.48
Xiaoheba	977.88	−1.69	432.49	1.16	232.18	**−2.11**	178.27	0.46	138.31	**−1.49**
Wusheng	856.54	−3.27	478.91	−1.21	205.11	**−1.90**	196.56	−0.82	132.45	**−1.24**
Luoduxi	1113.65	0.48	512.33	**4.48**	305.97	**−2.66**	210.33	**2.31**	170.30	**−2.17**

Note: the data in bold in β columns indicate that the trend is statistically significant (pass the trend test at $a = 0.05$ significance level). The following tables are similar.

Table 3
The observed area-averaged river discharge and its trends in the upper Yangtze River

Gauges	Annual		Summer		Autumn		Jul		Sep	
	Mean (mm)	β (mm/a)	Mean (mm)	β (mm/a)	Mean (mm)	β (mm/a)	Mean (mm)	β (mm/a)	Mean (mm)	β (mm/a)
Shigu	181.81	0.09	85.08	−0.12	59.33	0.05	32.76	0.01	30.71	−0.02
Pingshan	313.30	0.52	139.62	0.27	114.23	0.14	54.89	0.35	56.11	0.16
Zhutuo	384.41	−0.01	177.49	0.05	128.05	−0.21	70.11	0.19	62.35	0.01
Cuntan	399.34	−0.75	185.08	−0.01	133.47	**−0.68**	75.89	0.09	65.72	**−0.31**
Yichang	434.92	−0.31	197.10	**0.49**	141.31	**−0.73**	80.42	**0.42**	66.62	**−0.42**
Huning	392.24	0.45	191.68	0.27	137.31	0.19	78.03	0.27	69.31	0.13
Gaochang	647.77	−1.44	316.82	−0.88	195.14	**−0.76**	124.34	−0.52	95.25	−0.31
Lijiawan	523.53	**−4.03**	295.00	−2.33	154.54	**−1.31**	122.55	**−1.37**	86.90	**−0.72**
Beibei	424.55	**−3.65**	198.24	−0.09	142.84	**−2.71**	91.66	−0.05	75.31	**−1.60**
Wulong	608.88	1.27	285.98	2.79	140.02	**−0.62**	110.72	1.59	55.40	−0.11
Xiaoheba	495.35	−3.78	243.78	−1.94	158.42	**−1.80**	103.10	−1.24	88.21	**−1.21**
Wusheng	324.15	**−4.30**	143.27	−1.06	110.75	**−2.49**	65.57	−0.60	58.22	**−1.34**
Luoduxi	586.13	**−2.53**	270.63	**3.05**	200.34	**−3.93**	130.51	**1.67**	104.27	**−2.52**

given as a constant soil water content for the rainfall cases. During the non-rainfall period, evaporation from the soil surface exists, and the upper boundary condition is given as a constant flux. The soil water distribution along the hillslope is treated as uniform. The surface runoff is from the infiltration excess and saturation excess calculated by solving Richards' equation. The surface runoff flows through the hillslope into the stream by a kinematic wave. The groundwater aquifer is treated as an individual storage corresponding to each grid. The exchange between the groundwater and the river water is considered as a steady flow and is calculated by Darcy's law (Yang et al., 2002, 2004). The runoff generated from the grid is the lateral inflow into the river at the same flow interval. Flow routing in the river network is solved using the kinematic wave approach.

Extractions, diversions and reservoir operations are not accounted for in the hydrological model. Consequently, the simulated flows are natural flows that are different from the measured river discharges in artificial regulated rivers. However, the simulated river discharges offer a fundamental assessment of the available freshwater resources and the regulation extent of the river.

4.2. Model calibration and validation

The parameters used in the model include vegetation parameters, hillslope surface roughness, soil–water properties, river channel roughness, a snowmelting parameter and a groundwater parameter. Since most of the parameters have their physical meaning, they can be estimated through field tests. However, for such a large basin it is impossible

Please cite this article as: Xu, J., et al., Spatial and temporal variation of runoff in the Yangtze River basin during the past 40 years. Quaternary International (2007), doi:10.1016/j.quaint.2007.10.014

to measure all the parameters. Therefore, this study specifies the model parameters by referring to the existing database and handbooks.

A 5-year test run from 1961 to 1965 is carried out for calibrating the model parameters. One of the calibrated parameters in this model is the snowmelt factor in the temperature-based snowmelt equation. Another calibrated parameter, the hydraulic conductivity of the groundwater, is calibrated by checking the base flow in different sub-basins. Model validation is carried out from 1966 to 1970. In the calibration period, the Nash–Sutcliffe coefficient R^2 for the simulated daily discharges at the gauges on the mainstream is larger than 0.85, and the absolute values of the relative error (RE) are less than 5%. For the major tributaries, the model performance is slightly reduced; however, the values of R^2 are still larger than 0.75, and the absolute values of the RE are less than 8% (see Table 4 for details).

Table 4
Model performance in the calibration and validation periods

Gauges	Calibration (1966–1970)		Validation (1966–1970)	
	Relative error RE (%)	Nash coefficient R^2	Relative error RE (%)	Nash coefficient R^2
Shigu	−1.1	0.909	−5.5	0.847
Pingshan	1.6	0.919	−1.8	0.906
Zhutuo	0.7	0.930	5.0	0.925
Cuntan	0.6	0.921	−2.4	0.898
Yichang	1.5	0.853	−1.5	0.851
Huning	−6.2	0.911	−5.0	0.900
Gaochang	−7.4	0.862	2.9	0.854
Lijiawan	4.9	0.787	3.6	0.751
Beibei	−2.0	0.816	−7.6	0.791
Wulong	−4.4	0.812	−5.8	0.753
Xiaoheba	1.6%	0.766	−2.5%	0.765
Wusheng	−2.8%	0.807	−5.8%	0.812
Luoduxi	0.6%	0.793	−1.7%	0.732

5. Discussion

5.1. Changes in river discharge of the mainstream and major tributaries

According to simulated results, the trends in annual river discharges during 1961–2000 at three gauges located on the mainstream, namely Zhutuo, Cuntan and Yichang, are consistent with the observational trends shown in Table 3. This means that currently human activities have minor effects on the whole upper Yangtze River basin. As for the Pingshan gauge (Jinshajiang, see Tables 2, 3 and 5), both the observed and the simulated river discharges show an increasing trend (not significant at an $a = 0.05$ significance level) while the precipitation has a significant increasing trend. The simulated actual evapotranspiration in Jinshajiang is also increased (not significant, see Table 6). It was also found that the extent of trends in simulated and observed annual discharges at Pingshan are close (0.51 and 0.52, respectively). This illustrates that the change in the annual river runoff in the Jinshajiang tributary may be caused by the land use/cover change and/or increase of air temperature instead of the hydraulic structures on the river. The changes in land use and air temperature can change the evapotranspiration. Zhang et al. (2006b) also found that the runoff changes at the Pingshan gauge showed a mild increasing trend (not significant at a >95% confidence level), and suggested that annual runoff changes are mainly influenced by natural factors. Lu et al. (2003) indicated the land use changes and other human activities also played a role in the river discharge changes. A similar situation can also be found at the Shigu gauge.

For the Yichang gauge, the observed annual precipitation (see Table 2), river discharge (see Table 3) and simulated river discharge (see Table 5) have close non-significant downward trends (−0.31 to −0.51 mm/a). In summer, the observed river discharge has a significant increasing trend with a slope of $\beta = 0.49$ mm/a (see Table 3), which is

Table 5
The simulated area-averaged river discharge and its trends in the upper Yangtze River

Gauges	Annual		Summer		Autumn		Jul		Sep	
	Mean (mm)	β (mm/a)	Mean (mm)	β (mm/a)	Mean (mm)	β (mm/a)	Mean (mm)	β (mm/a)	Mean (mm)	β (mm/a)
Shigu	179.93	0.04	90.22	−0.38	61.81	0.25	35.59	−0.06	32.62	0.09
Pingshan	303.95	0.51	135.13	0.00	103.97	0.33	52.35	0.16	51.19	0.21
Zhutuo	388.94	−0.19	187.32	−0.29	121.28	0.05	70.48	0.04	61.88	0.07
Cuntan	401.88	−0.57	188.35	−0.08	127.73	**−0.37**	72.93	0.15	64.70	−0.19
Yichang	431.51	−0.50	202.24	0.27	131.41	**−0.44**	78.18	**0.34**	64.15	**−0.21**
Huning	378.37	0.92	177.22	0.24	129.56	0.50	72.69	0.23	66.12	0.28
Gaochang	620.23	−1.65	325.42	−0.99	164.26	−0.28	116.49	−0.35	88.70	−0.10
Lijiawan	549.33	**−2.96**	316.33	−1.77	158.20	**−1.54**	122.99	−0.67	96.90	**−0.88**
Beibei	427.28	−1.96	178.34	0.60	148.05	**−1.92**	77.47	**0.50**	76.43	**−1.21**
Wulong	648.22	−0.22	339.22	2.68	152.25	**−0.98**	123.97	1.65	57.93	−0.09
Xiaoheba	511.18	−1.73	167.42	1.02	149.70	**−2.03**	73.66	**0.70**	75.16	**−1.29**
Wusheng	417.65	−3.39	209.07	−1.12	142.27	**−1.79**	87.46	−0.29	82.17	**−1.11**
Luoduxi	633.43	0.99	257.26	**4.23**	224.03	**−2.43**	115.23	**2.58**	109.30	**−1.71**

Table 6
The simulated area-averaged actual evapotranspiration and its trends in the upper Yangtze River

Gauges	Annual		Summer		Autumn		Jul		Sep	
	Mean (mm)	β (mm/a)	Mean (mm)	β (mm/a)	Mean (mm)	β (mm/a)	Mean (mm)	β (mm/a)	Mean (mm)	β (mm/a)
Shigu	324.90	0.73	143.50	0.12	90.46	0.05	51.04	0.06	41.26	−0.06
Pingshan	366.95	0.51	139.42	−0.02	104.31	0.02	48.67	−0.04	42.29	−0.08
Zhutuo	379.39	0.34	145.98	−0.05	101.38	0.00	51.22	−0.06	41.82	−0.06
Cuntan	397.88	0.21	158.73	−0.14	100.21	0.04	55.88	**−0.10**	42.62	−0.02
Yichang	407.78	0.10	164.26	−0.25	101.17	0.05	58.35	**−0.16**	43.95	−0.02
Huning	384.83	0.33	142.79	−0.14	109.38	−0.03	49.65	−0.07	41.79	−0.10
Gaochang	398.48	0.11	156.79	−0.08	94.37	−0.02	54.82	−0.06	39.22	−0.03
Lijiawan	425.00	−0.51	177.05	−0.16	81.56	−0.09	63.99	−0.11	38.57	−0.01
Beibei	460.85	−0.06	202.40	**−0.30**	95.22	0.20	70.74	−0.15	44.27	**0.13**
Wulong	479.28	−0.32	186.97	**−0.79**	109.37	0.19	70.48	**−0.55**	53.40	−0.02
Xiaoheba	467.05	−0.03	207.75	**−0.34**	97.12	0.22	72.50	**−0.17**	45.36	**0.14**
Wusheng	439.60	−0.01	183.51	−0.07	89.93	0.15	63.91	−0.02	40.72	**0.11**
Luoduxi	479.29	−0.63	214.55	**−0.89**	95.33	0.19	75.37	**−0.41**	45.39	**0.16**

larger than the changing slopes of precipitation and simulated river discharge. The changes in land use and river flood plain may be the main factors for the river discharge increase in the flood season. However, in autumn, the observed river discharge significantly declined with a slope of $\beta = -0.73$ mm/a, which is also larger than the changing slopes of precipitation ($\beta = -0.52$ mm/a) and simulated river discharge ($\beta = -0.44$ mm/a). It is believed that, besides the reduction in precipitation in autumn, the water consumption and reservoir storage may contribute to the decrease in river discharge. The increasing discharge in summer, particularly in July, would bring more floods flowing into the Three Gorges reservoir, and the decreasing discharge in September and October would influence the power generation when the reservoir begins to store.

However, in tributaries and their branches, the river routings have been disturbed gradually by the hydraulic structures. In the Jialingjiang tributary and its branches, the annual river discharges observed at the Beibei, Wusheng and Luoduxi gauges declined significantly with $\beta = -2.53$ to -14.30 mm/a (see Table 3), but with no significant decreasing trend in the precipitation, simulated river discharge and evapotranspiration. Moreover, the declining slope β of the observed river discharge in the Jialingjiang tributary and its branches in autumn is larger than the simulated values and precipitation. Both of these demonstrate that the decrease in river discharge in Jialingjiang is mainly due to human activities, e.g. water consumption. In July, the main flooding month, the simulated monthly river discharges at Beibei and Xiaoheba increase significantly with $\beta = 0.5$–0.7 mm/a (see Table 5), but a slightly decreasing trend (not significant) is found in the observed discharges. This is speculated to be predominantly influenced by reservoir regulation or irrigation water intake. In September, both simulated and observed river discharges at the Biebei, Xiaoheba, Wusheng and Luoduxi gauges have significant decreasing trends (see Tables 3 and 5), which can be deduced to be due to the decrease in precipitation (see Table 2) and the increase in evapotranspiration (see Table 6).

5.2. Changes in spatial distribution of runoff over the upper basin

By means of hydrological modeling, except for river discharge, it is easy to obtain the daily spatial distribution of runoff depth, which aids our understanding of the distributed characteristics of runoff. For example, Fig. 4 shows the seasonal distribution of runoff depth. In winter, the runoff concentrates in the middle-lower Jinshajiang (west-southern region of the upper Yangtze) and the mountainous area around the Sichuan basin. In spring, Jinshajiang, west and east of Sichuan basin, and Wujiang are the main regions where the runoff is generated. In summer, owing to rainstorms, the runoff is generated in the west and east of the Sichuan basin, Three Gorges region and Wujiang tributary. In a flood year, the runoff generated in summer can be close to 60–80% of the annual total. The distribution of autumnal runoff is spatially slightly even.

The change trend of seasonal runoff ratios (ratio = $(R_{\text{seasonal}}/R_{\text{annual}}) \times 100\%$) in each grid has also been detected using the TFPW-MK method with a significance level of $a = 0.05$. In the east of the Sichuan basin, it is found that there are significant trends, i.e., increasing in summer and decreasing in autumn (see Fig. 5). For example in the 1990s, the seasonal runoff ratio increased about 10% in summer but decreased 10–20% in autumn compared with the period of 1961–1990.

6. Conclusions

The paper firstly analyzed the trends in precipitation and observed river discharge in the whole Yangtze River basin by means of a TFPW-MK test. It was found that the

Please cite this article as: Xu, J., et al., Spatial and temporal variation of runoff in the Yangtze River basin during the past 40 years. Quaternary International (2007), doi:10.1016/j.quaint.2007.10.014

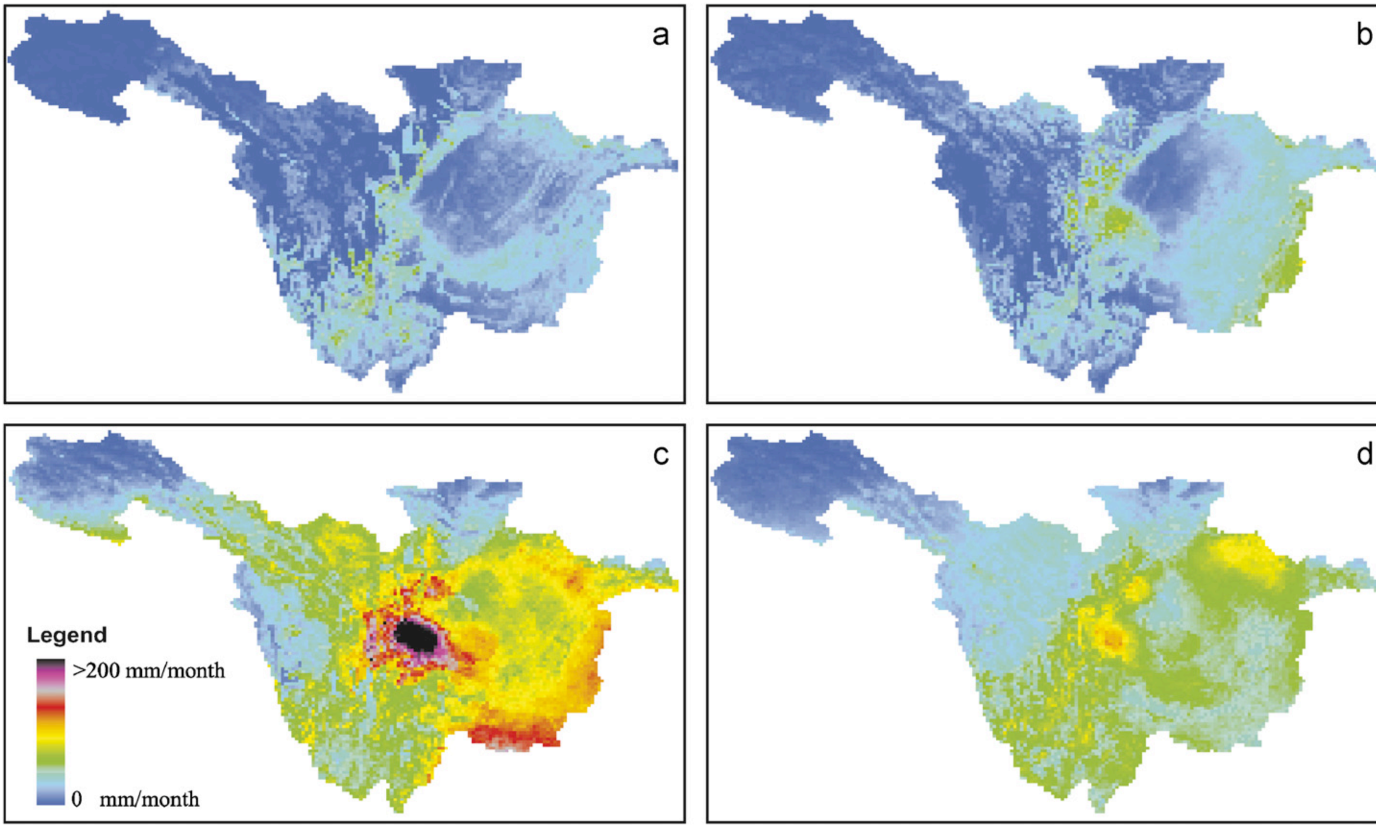

Fig. 4. Seasonal distribution of runoff depth during 1961–2000: (a) in winter, (b) in spring, (c) in summer and (d) in autumn.

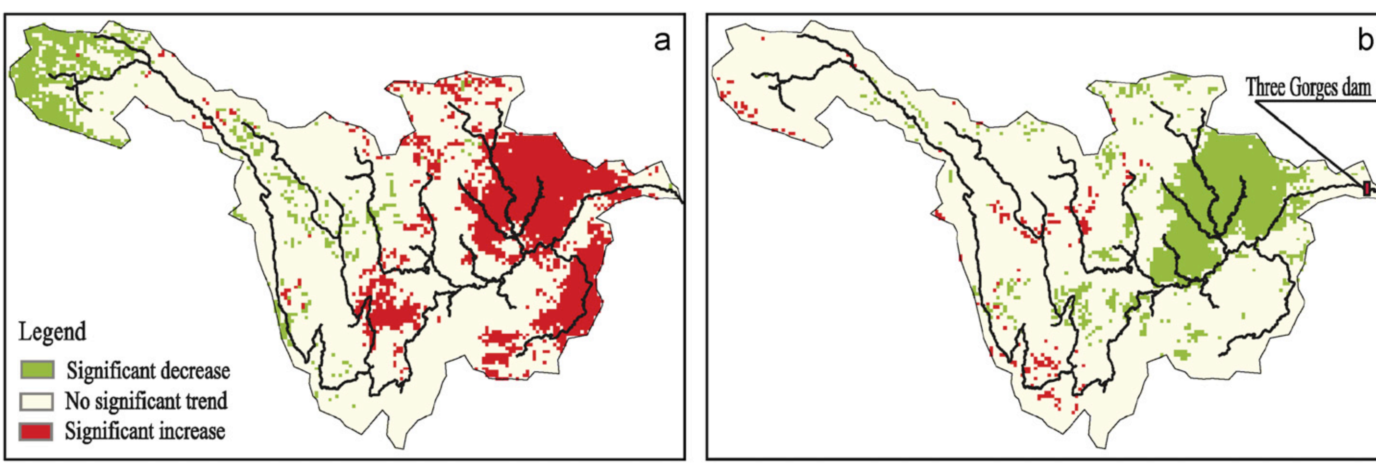

Fig. 5. Trends in the seasonal runoff ratio during 1961–2000: (a) in summer and (b) in autumn.

spatial and temporal distributions of precipitation had significant variations. The increased precipitation was concentrated in the middle and lower reaches of the Yangtze River in summer, which has brought about several flood disasters. However, in the upper reach of the Three Gorges Dam site, the precipitation had a significant decreasing trend in the non-flooding season (autumn), and this possibly resulted in more frequent or extreme droughts, particularly in spring and autumn. The serious drought that occurred in the Chongqing municipality and the Sichuan province in 2006 may be associated with this changing trend. As for the Three Gorges reservoir, an increasing trend of discharge in the upstream in July, which is the main flooding month, would bring more flood water flowing into the reservoir, and a decreasing trend in September and October, which is the start of reservoir storage, would not benefit water storage and power generation. In the trend analysis, it was also found that the trends in precipitation and river discharge did not match, particularly in some tributaries and smaller branches where the impact of reservoirs on river discharge could not be neglected.

To better understand the natural hydrological response to the variation in climate, a distributed hydrological model was employed for simulating the natural river runoff in the upper Yangtze River basin. Comparing the simulated river discharge with the observed one, the impacts on the river discharge by climatic factors and human activity were clearly distinguished. Changes of annual river discharge on the mainstream were predominantly due to climate variability, e.g. precipitation and evapotranspiration. However, the changes in seasonal and monthly river discharge for some tributaries were deduced to be mainly due to human activities, e.g. reservoir regulation and irrigation. Moreover, in the east of the Sichuan province, it was found that the seasonal runoff ratio increased in summer but decreased greatly in autumn.

Although there lacked sufficient validation in the simulated grid, the distributed physically based hydrological model offered considerable information on the spatial and temporal distributions of runoff and evapotranspiration, which were useful for water resource assessment as well as for understanding the basin hydrological characteristics. The model results showed that the seasonal runoff distribution had significant variability in the upper Yangtze River basin due to the precipitation increase in summer and decrease in autumn. This natural trend implies that there is a forewarning of increasing floods in summer and water shortage in autumn in the upper Yangtze River.

Acknowledgements

This research was supported mainly by the national "948" project (Contract no. 200760) funded by the Ministry of Water Resources and partially by the Commonweal Fund (YWF0713/ZY05) from the Changjiang Scientific Research Institute of CWRC. The reviewers' comments are gratefully acknowledged.

References

Becker, S., Gemmer, M., Jiang, T., 2006. Spatiotemporal analysis of precipitation trends in the Yangtze River catchment. Stochastic Environmental Research and Risk Assessment (SERRA) 20, 435–444.

Chen, X., Zong, Y., Zhang, E., Xu, J., Li, S., 2001. Human impacts on the Changjiang (Yangtze) River basin, China, with special reference to the impacts on the dry season water discharges into the sea. Geomorphology 41, 111–123.

Doll, P., Kaspar, F., Lehner, B., 2003. A global hydrological model for deriving water availability indicators: model tuning and validation. Journal of Hydrology 270, 105–134.

Gemmer, M., Becker, S., Jiang, T., 2004. Observed monthly precipitation trends in China 1951–2002. Theoretical and Applied Climatology 77, 39–45.

Houghton, J., Ding, Y., Griggs, D., Noguer, M., Van Der Linden, P., Xiaosu, D., Makdell, K., Johnson, C. (Eds.), 2001. Climate Change: The Scientific Basis. Third Assessment Report of the Intergovernmental Panel on Climate Change. Cambridge University Press, Cambridge.

Jiang, T., Su, B., Hartmann, H., 2007. Temporal and spatial trends of precipitation and river flow in the Yangtze River basin, 1961–2000. Geomorphology 85, 143–154.

Kulkarni, A., von Storch, H., 1995. Monte Carlo experiments on the effect of serial correlation on the Mann–Kendall test of trend. Meteorologische Zeitschrift 4 (2), 82–85.

Lu, X., 2005. Spatial variability and temporal change of water discharge and sediment flux in the lower Jinsha tributary: impact of environmental changes. River Research and Application 21, 229–243.

Lu, X., Ashmore, P., Wang, J., 2003. Seasonal water discharge and sediment load changes in the upper Yangtze, China. Mountain Research and Development 23 (1), 56–64.

Milly, P., Dunne, K., Vecchia, A., 2005. Global pattern of trends in streamflow and water availability in a changing climate. Nature 438, 347–350.

Oki, T., Agata, Y., Kanae, S., Saruhashi, T., Yang, D., Musiake, K., 2001. Global assessment of current water resources using total runoff integrating pathways. Hydrological Sciences Journal 46 (6), 983–995.

Refsgaard, J., 1996. Terminology, modeling protocol and classification of hydrological model codes. In: Abbott, M., Refsgaard, J. (Eds.), Distributed Hydrological Modeling. Kluwer Academic Publisher, Dordrecht.

Su, B., Jiang, T., 2006. Recent trends in temperature and precipitation extremes in the Yangtze River basin, China. Theoretical and Applied Climatology 83 (1–4), 139–151.

Trenberth, K., Dai, A., Rasmussen, R., Parsons, D., 2003. The changing character of precipitation. Bulletin of American Meteorology Society 84, 1205–1217.

Yang, D., Herath, S., Musiake, K., 1998. Development of a geomorphology-based hydrological model for large catchments. Annual Journal of Hydraulic Engineering, JSCE 42, 169–174.

Yang, D., Musiake, K., Kanae, S., Oki, T., 2000. Use of the Pfafstetter basin numbering system in hydrological modeling. In: Proceedings of the 2000 Annual Conference, Japan Society of Hydrology and Water Resources, pp. 200–201.

Yang, D., Herath, S., Musiake, K., 2002. A Hillslope-based hydrological model using catchment area and width function. Hydrological Sciences Journal 47 (1), 49–65.

Yang, D., Li, C., Ni, G., Hu, H., 2004. Application of a distributed hydrological model to the Yellow River basin. Acta Geographica Sinica 59 (1), 143–154.

Yue, S., Wang, C., 2002. Applicability of prewhitening to eliminate the influence of serial correlation on the Mann–Kendall test. Water Resources Research 38 (6), 1068.

Yue, S., Pilon, P., Phinney, B., Cavadias, G., 2002. The influence of autocorrelation on the ability to detect trend in hydrological series. Hydrological Processes 16 (9), 1807–1829.

Zhang, Q., Jiang, T., Gemmer, M., Becker, S., 2005. Precipitation, temperature and runoff analysis from 1950 to 2002 in the Yangtze catchment, China. Hydrological Sciences Journal 50 (1), 65–80.

Zhang, Q., Liu, C., Xu, C., Xu, Y., Jiang, T., 2006a. Observed trends of annual maximum water level and streamflow during past 130 years in the Yangtze River basin, China. Journal of Hydrology 324, 255–265.

Zhang, Q., Xu, C., Becker, S., Jiang, T., 2006b. Sediment and runoff changes in the Yangtze River basin during past 50 years. Journal of Hydrology 331, 511–523.